



Heat and Mass Transfer Analysis of a Three-Dimensional MHD Convective Flow with Sinusoidal Suction in the Presence of Radiation Absorption and Diffusion Thermo Effect

Nazibuddin Ahmed¹ · Dipunja Gohain¹

Accepted: 10 November 2023 / Published online: 9 December 2023
© The Author(s), under exclusive licence to Springer Nature India Private Limited 2023

Abstract

The significance of the radiation absorption effect on MHD flow and heat transfer problems has become more important in many industrial applications. Particularly at a high operating temperature, the radiation effect becomes quite significant. Therefore, the primary motive of the current study is to explore the radiation absorption effect along with the diffusion thermo effect on a three-dimensional MHD convective flow of a radiating fluid in the presence of sinusoidal suction. To derive the non-dimensional governing equations, the regular perturbation approach is employed. The effect of various rheological parameters on the velocity, temperature, and concentration fields, as well as skin friction, the Nusselt number, and the Sherwood number, is depicted graphically. Finally, it is highlighted that both radiation absorption and the Dufour effect contribute to the enhancement of shear stress and heat transfer rate at the plate. Furthermore, it has been established that increasing the Reynolds number decelerates the momentum transfer rate while enhancing both the heat and mass transfer rates.

Keywords MHD · Diffusion-thermo (Dufour effect) · Radiation-absorption · Sinusoidal suction · Perturbation method

Mathematics Subject Classification 76W05 · 80A19

List of Symbols

\vec{B}	Magnetic flux density
B_0	Strength of uniform magnetic field
C	Molar species concentration
C_p	Specific heat at constant pressure
C_∞	Free stream concentration
p_∞	Free stream pressure
C_w	Concentration at the wall

✉ Dipunja Gohain
dipunja31@gauhati.ac.in

¹ Department of Mathematics, Gauhati University, Guwahati, Assam 781014, India

D_M	Mass diffusivity
K_T	Thermal diffusion ratio
\vec{E}	Electric field
Du	Dufour parameter
p	Pressure
g	Acceleration due to gravity
Gr	Thermal Grashof number
\vec{J}	Current density
k^*	Mean absorption constant
M	Magnetic field parameter
N	Radiation parameter
Gm	Solutal Grashof number
Re	Reynolds number
Pr	Prandtl number
Q_l	Radiation absorption parameter
\vec{q}_r	Radiative heat flux vector
Sc	Schmidt number
\bar{t}	Time
t_0	Characteristics time
T	Fluid temperature
T_w	Temperature at the wall
T_∞	Undisturbed temperature
u	X-component of fluid velocity
v	Y-component of fluid velocity
w	Z-component of fluid velocity
U	Uniform plate velocity
γ	Chemical reaction parameter
σ	Electrical conductivity
σ^*	Stephan–Boltzmann constant
μ	Dynamic viscosity
β	Volumetric coefficient of thermal expansion
$\bar{\beta}$	Volumetric coefficient of solutal expansion
ν	Kinematic Viscosity
κ	Thermal conductivity
w	Conditions at the plate
∞	Conditions at infinity

Introduction

During the last few decades, investigators have paid close curiosity to the study of coupled heat and mass transfer flow. This is mostly due to its various applications in the scientific, technical, and industrial sectors. These applications cover a wide range of topics, including chemical processing machinery, oceanic circulation, emergency cooling systems of advanced nuclear reactors, cooling techniques for plastic sheets, fog formation and dissipation, food processing and drying, temperature distribution, moisture control in agricultural fields, and polymer production. A huge volume of studies has been conducted on different aspects of heat and mass transfer with the MHD effect, a few of them are Riaz et al. [1], Javaherdeh

et al. [2], Mahanthesh et al. [3], Kataria and Patel [4], Chamkha and Rashad [5], Krishna et al. [6] etc.

A few other works that addressed the three-dimensional MHD convective flow together with sinusoidal suction velocity under various physical situations can be found in Ahmed [7], Zafar et al. [8], Rana et al. [9], Jain and Gupta [10], Rana and Latif [11] etc.

The importance of radiation absorption on the flow of fluids is quite relevant from the perspective of science. Such a phenomenon has been detected in planetary atmospheres while absorbing radiation from neighbouring stars. Additionally, this effect is significant in many industrial applications, encompassing oil reservoirs, thermal insulation, catalytic reactors, reactor safety measures, geothermal systems, etc. To emphasize the relevance of the effects caused by radiation absorption, numerous articles have been published, for instance, Ibrahim et al. [12], Narayana [13], Hernandez and Zueco [14], Venkateswarlu and Narayana [15], Krishna [16] and Azifuzzaman et al. [17]. Convective flow with thermal radiation occurs in many industrial processes, including heating or cooling chambers, energy operations, evaporation from vast reservoirs, solar power technologies, etc. Recently, Anwar et al. [18], Asifa et al. [19], Anwar et al. [20], Wahid et al. [21], and Anwar et al. [22] examined the free convective flow of a radiating fluid in the presence of a magnetic field.

Despite being of lesser magnitude than the effects defined by Fourier’s and Fick’s laws, the Dufour and Soret effects often go unnoticed in several studies. However, there are many scenarios where exceptions are made. The Dufour effect is essential and unavoidable in several instances, as reported by Eckert and Drake [23]. Studies such as Waini et al. [24], Postelnicu [25], and Kandasamy et al. [26], Kune et al. [27], Zhao et al. [28], Huang and Yih [29] and Reddy et al. [30] delved into various facets of the Dufour effect.

The main goal of the current study is to investigate the three-dimensional MHD mixed convective flow of a radiating fluid with sinusoidal suction velocity, radiation absorption, and the Dufour effect. Numerous publications that have examined different facets of the radiation absorption effect may have been discovered up to this point. However, to our knowledge, none of the research to date has looked at how radiation absorption and diffusion-thermo affect the three-dimensional heat and mass transfer flow of a radiating fluid with sinusoidal suction. The consideration of the radiation absorption effect on a three-dimensional flow with sinusoidal suction velocity makes our problem differ from any other previously existing model, which is also the novelty of the present study.

Basic Equations

The equations for the steady, incompressible, viscous, electrically conducting radiating fluid over an infinite vertical plate under the influence of diffusion-thermo and radiation absorption effects are as follows:

Mass continuity equation (Ahmed [7]):

$$\vec{\nabla} \cdot \vec{q} = 0. \tag{1}$$

Momentum equation (Ahmed [7]):

$$\left(\vec{q} \cdot \vec{\nabla}\right)\vec{q} = -\frac{1}{\rho}\vec{\nabla} p + \nu\nabla^2\vec{q} + \frac{\vec{J} \times \vec{B}}{\rho} + \vec{g}. \tag{2}$$

Energy equation (Ahmed [7]):

$$\rho C_p (\vec{q} \cdot \vec{\nabla}) T = \kappa \nabla^2 T + \frac{\rho D_M K_T}{C_S} \nabla^2 C - \vec{\nabla} \cdot \vec{q}_r + \bar{Q}(C - C_\infty). \tag{3}$$

Species continuity equation (Ahmed [7]):

$$(\vec{q} \cdot \vec{\nabla}) C = D_M \nabla^2 C - \bar{K}(C - C_\infty). \tag{4}$$

Ohm’s Law for moving conductor:

$$\vec{J} = \sigma (\vec{E} + \vec{q} \times \vec{B}). \tag{5}$$

All the symbols are provided in the nomenclature section.

Problem Formulation

Consider a steady three-dimensional convective hydromagnetic flow of a viscous, incompressible, electrically conducting fluid past a semi-infinite vertical plate. A coordinate reference frame is introduced in which the \bar{x} -axis is set parallel to the plate, the \bar{y} -axis is orthogonal to the plate, and the \bar{z} -axis is orthogonal to the \bar{x} - \bar{y} plane. Let $\vec{q} = (\bar{u}, \bar{v}, \bar{w})$ be the fluid velocity and $\vec{B} = (0, B_0, 0)$ be the uniform magnetic field imposed orthogonal to the plate. Figure 1 portrays the physical model of the flow problem.

Our study is confined to the assumptions listed below:

1. Except for the density in the buoyancy force term, all fluid properties are taken to be constant.
2. No external electric field is taken into account.
3. It is presumed that the plate is electrically non-conducting.
4. $T_w > T_\infty$ and $C_w > C_\infty$.
5. It is assumed that the magnetic Reynolds number is sufficiently low so that the effect of the induced magnetic field is considered negligible when compared to the applied magnetic field.

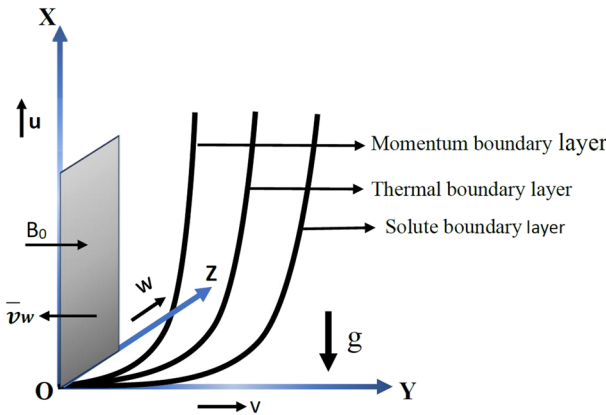


Fig. 1 Schematic diagram of the problem

The plate experiences a sinusoidal suction velocity defined by

$$\bar{v}_w = -V_0 \left(1 + \epsilon \cos \frac{\pi \bar{z}}{L} \right) \tag{6}$$

where $V_0 > 0$ is the undisturbed part of the suction velocity, L is the wavelength of the periodic suction, and $\epsilon (\ll 1)$ is the amplitude of the suction velocity.

Based on the previously mentioned assumptions and utilizing the Boussinesq approximations, Eqs. (1–4) can be simplified to the following expression:

Equation of continuity:

$$\frac{\partial \bar{v}}{\partial \bar{y}} + \frac{\partial \bar{w}}{\partial \bar{z}} = 0. \tag{7}$$

Momentum equations:

$$\bar{v} \frac{\partial \bar{u}}{\partial \bar{y}} + \bar{w} \frac{\partial \bar{u}}{\partial \bar{z}} = g\beta(T - T_\infty) + g\bar{\beta}(C - C_\infty) + \nu \left(\frac{\partial^2 \bar{u}}{\partial \bar{y}^2} + \frac{\partial^2 \bar{u}}{\partial \bar{z}^2} \right) - \frac{\sigma B_0^2 \bar{u}}{\rho}, \tag{8}$$

$$\bar{v} \frac{\partial \bar{v}}{\partial \bar{y}} + \bar{w} \frac{\partial \bar{v}}{\partial \bar{z}} = -\frac{1}{\rho} \frac{\partial \bar{p}}{\partial \bar{y}} + \nu \left(\frac{\partial^2 \bar{v}}{\partial \bar{y}^2} + \frac{\partial^2 \bar{v}}{\partial \bar{z}^2} \right), \tag{9}$$

$$\bar{v} \frac{\partial \bar{w}}{\partial \bar{y}} + \bar{w} \frac{\partial \bar{w}}{\partial \bar{z}} = -\frac{1}{\rho} \frac{\partial \bar{p}}{\partial \bar{z}} + \nu \left(\frac{\partial^2 \bar{w}}{\partial \bar{y}^2} + \frac{\partial^2 \bar{w}}{\partial \bar{z}^2} \right) - \frac{\sigma B_0^2 \bar{w}}{\rho}. \tag{10}$$

Energy equation:

$$\begin{aligned} \bar{v} \frac{\partial T}{\partial \bar{y}} + \bar{w} \frac{\partial T}{\partial \bar{z}} &= \frac{\kappa}{\rho C_p} \left(\frac{\partial^2 T}{\partial \bar{y}^2} + \frac{\partial^2 T}{\partial \bar{z}^2} \right) + \frac{D_M K_T}{C_S C_p} \left(\frac{\partial^2 C}{\partial \bar{y}^2} + \frac{\partial^2 C}{\partial \bar{z}^2} \right) \\ &\quad - \frac{1}{\rho C_p} \vec{\nabla} \cdot \vec{q}_r + \frac{\bar{Q}}{\rho C_p} (C - C_\infty). \end{aligned} \tag{11}$$

Species continuity equation:

$$\bar{v} \frac{\partial C}{\partial \bar{y}} + \bar{w} \frac{\partial C}{\partial \bar{z}} = D_M \left(\frac{\partial^2 C}{\partial \bar{y}^2} + \frac{\partial^2 C}{\partial \bar{z}^2} \right) - \bar{K} (C - C_\infty). \tag{12}$$

By employing the Rosseland approximation (cite{venkateswarlu2015}), the radiative heat flux \vec{q}_r can be determined for an optically thick non-gray gas by the following expression:

$$\vec{q}_r = -\frac{4\sigma^*}{3\kappa^*} \vec{\nabla} T^4. \tag{13}$$

Since, within the fluid flow $|T - T_\infty| \ll 1$, therefore T^4 can be expressed as

$$T^4 = \{T_\infty + (T - T_\infty)\}^4 \approx 4TT_\infty^3 - 3T_\infty^4. \tag{14}$$

Utilizing the Eqs. (13) and (14), Eq. (11) transforms to

$$\begin{aligned} \bar{v} \frac{\partial T}{\partial \bar{y}} + \bar{w} \frac{\partial T}{\partial \bar{z}} &= \frac{\kappa}{\rho C_p} \left(\frac{\partial^2 T}{\partial \bar{y}^2} + \frac{\partial^2 T}{\partial \bar{z}^2} \right) + \frac{D_M K_T}{C_S C_p} \left(\frac{\partial^2 C}{\partial \bar{y}^2} + \frac{\partial^2 C}{\partial \bar{z}^2} \right) \\ &\quad + \frac{16\sigma^* T_\infty^3}{3\kappa^* \rho C_p} \nabla^2 T + \frac{\bar{Q}}{\rho C_p} (C - C_\infty). \end{aligned} \tag{15}$$

The appropriate boundary conditions for the given problem are as follows (Ahmed [7])

$$\bar{u} = U, \quad \bar{v} = \bar{v}_w, \quad \bar{w} = 0, \quad T = T_w, \quad C = C_w \quad \text{at} \quad \bar{y} = 0 \tag{16}$$

$$\bar{u} \rightarrow 0, \quad \bar{v} \rightarrow -V_0, \quad \bar{w} \rightarrow 0, \quad T \rightarrow T_\infty, \quad C \rightarrow C_\infty, \quad \bar{p} \rightarrow \bar{p}_\infty \quad \text{as } \bar{y} \rightarrow \infty \quad (17)$$

Some dimensionless quantities are introduced as follows

$$y = \frac{\bar{y}}{L}, \quad z = \frac{\bar{z}}{L}, \quad u = \frac{\bar{u}}{U}, \quad v = \frac{\bar{v}}{V_0}, \quad w = \frac{\bar{w}}{V_0}, \quad \theta = \frac{T - T_\infty}{T_w - T_\infty}, \quad \phi = \frac{C - C_\infty}{C_w - C_\infty},$$

$$\text{Pr} = \frac{\mu C_p}{\kappa}, \quad \text{Sc} = \frac{\nu}{D_M}, \quad \text{Du} = \frac{K_T D_M (C - C_\infty)}{\nu C_s C_p (T_w - T_\infty)},$$

$$\text{Gr} = \frac{L g \beta (T_w - T_\infty)}{U V_0}, \quad \text{Gm} = \frac{L g \bar{\beta} (C_w - C_\infty)}{U V_0},$$

$$M = \frac{\sigma B_0^2 \nu}{\rho V_0^2}, \quad \text{Re} = \frac{V_0 L}{\nu}, \quad N = \frac{\kappa \kappa^*}{4 \sigma^* T_\infty^3}, \quad Q_I = \frac{\bar{Q} L (C_w - C_\infty)}{\rho C_p V_0 (T_w - T_\infty)}, \quad \gamma = \frac{L \bar{K}}{V_0},$$

$$p = \frac{\bar{p}}{\rho \left(\frac{\nu}{L}\right)^2}, \quad p_\infty = \frac{\bar{p}_\infty}{\rho \left(\frac{\nu}{L}\right)^2}.$$

Based on the non-dimensional quantities, the Eqs. (7–10), (12), and (15) are reduced to

$$\frac{\partial v}{\partial y} + \frac{\partial w}{\partial z} = 0, \tag{18}$$

$$v \frac{\partial u}{\partial y} + w \frac{\partial u}{\partial z} = \text{Gr} \theta + \text{Gm} \phi + \frac{1}{\text{Re}} \left(\frac{\partial^2 u}{\partial y^2} + \frac{\partial^2 u}{\partial z^2} \right) - M \text{Re} u, \tag{19}$$

$$v \frac{\partial v}{\partial y} + w \frac{\partial v}{\partial z} = -\frac{1}{\text{Re}^2} \frac{\partial p}{\partial y} + \frac{1}{\text{Re}} \left(\frac{\partial^2 v}{\partial y^2} + \frac{\partial^2 v}{\partial z^2} \right), \tag{20}$$

$$v \frac{\partial w}{\partial y} + w \frac{\partial w}{\partial z} = -\frac{1}{\text{Re}^2} \frac{\partial p}{\partial z} + \frac{1}{\text{Re}} \left(\frac{\partial^2 w}{\partial y^2} + \frac{\partial^2 w}{\partial z^2} \right) - M \text{Re} w, \tag{21}$$

$$v \frac{\partial \theta}{\partial y} + w \frac{\partial \theta}{\partial z} = \frac{1}{\text{Pr Re}} \left(1 + \frac{4}{3N} \right) \left(\frac{\partial^2 \theta}{\partial y^2} + \frac{\partial^2 \theta}{\partial z^2} \right) + \frac{\text{Du}}{\text{Re}} \left(\frac{\partial^2 \phi}{\partial y^2} + \frac{\partial^2 \phi}{\partial z^2} \right) + Q_I \phi, \tag{22}$$

$$v \frac{\partial \phi}{\partial y} + w \frac{\partial \phi}{\partial z} = \frac{1}{\text{Sc Re}} \left(\frac{\partial^2 \phi}{\partial y^2} + \frac{\partial^2 \phi}{\partial z^2} \right) - \gamma \phi. \tag{23}$$

The corresponding boundary conditions are

$$u = 1, \quad v = -1 - \epsilon \cos \pi z, \quad w = 0, \quad \theta = 1 = \phi \quad \text{at } y = 0, \tag{24}$$

$$u \rightarrow 0, \quad v \rightarrow -1, \quad w \rightarrow 0, \quad \theta \rightarrow 0, \quad \phi \rightarrow 0, \quad p \rightarrow p_\infty \quad \text{as } y \rightarrow \infty. \tag{25}$$

Solution Methodology

To solve Eqs. (18–23), we assume the solution of the following form:

$$f(y, z) = f_0(y) + \epsilon f_1(y, z) + O(\epsilon^2). \tag{26}$$

where f stands for u, v, w, θ, ϕ and p with $p_0 = p_\infty$, and $w_0 = 0$. Substituting (26) into Eqs. (18–23) and equating the coefficients of ϵ^0 and ϵ , and ignoring the higher order terms of ϵ^2 , we have the following equations.

Zeroth-order equations:

$$\frac{dv_0}{dy} = 0, \tag{27}$$

$$v_0 \frac{du_0}{dy} = Gr \theta_0 + Gm \phi_0 + \frac{1}{Re} \frac{d^2 u_0}{dy^2} - M Re u_0, \tag{28}$$

$$v_0 \frac{d\theta_0}{dy} = \frac{1}{Pr Re} \left(1 + \frac{4}{3N} \right) \frac{d^2 \theta_0}{dy^2} + \frac{Du}{Re} \frac{d^2 \phi_0}{dy^2} + Q_I \phi_0, \tag{29}$$

$$v_0 \frac{d\phi_0}{dy} = \frac{1}{Sc Re} \frac{d^2 \phi_0}{dy^2} - \gamma \phi_0, \tag{30}$$

The corresponding zeroth order boundary conditions are

$$u_0 = 1, \quad v_0 = 0, \quad \theta_0 = 1 = \phi_0 \quad \text{at } y = 0, \tag{31}$$

$$u_0 = 0, \quad v_0 = -1, \quad \theta_0 = 0 = \phi_0 \quad \text{as } y \rightarrow \infty. \tag{32}$$

First-order equations:

$$\frac{\partial v_1}{\partial y} + \frac{\partial w_1}{\partial z} = 0, \tag{33}$$

$$-\frac{\partial u_1}{\partial y} + v_1 u_1' = Gr \theta_1 + Gm \phi_1 + \frac{1}{Re} \left(\frac{\partial^2 u_1}{\partial y^2} + \frac{\partial^2 u_1}{\partial z^2} \right) - M Re u_1, \tag{34}$$

$$-\frac{\partial v_1}{\partial y} = -\frac{1}{Re^2} \frac{\partial p_1}{\partial y} + \frac{1}{Re} \left(\frac{\partial^2 v_1}{\partial y^2} + \frac{\partial^2 v_1}{\partial z^2} \right), \tag{35}$$

$$-\frac{\partial w_1}{\partial z} = -\frac{1}{Re^2} \frac{\partial p_1}{\partial z} + \frac{1}{Re} \left(\frac{\partial^2 w_1}{\partial y^2} + \frac{\partial^2 w_1}{\partial z^2} \right) - M Re w_1, \tag{36}$$

$$-\frac{\partial \theta_1}{\partial y} + v_1 \theta_1' = \frac{\Lambda}{Re Pr} \left(\frac{\partial^2 \theta_1}{\partial y^2} + \frac{\partial^2 \theta_1}{\partial z^2} \right) + \frac{Du}{Re} \left(\frac{\partial^2 \phi_1}{\partial y^2} + \frac{\partial^2 \phi_1}{\partial z^2} \right) + Q_I \phi_1, \tag{37}$$

$$-\frac{\partial \phi_1}{\partial y} + v_1 \phi_1' = \frac{1}{Sc Re} \left(\frac{\partial^2 \phi_1}{\partial y^2} + \frac{\partial^2 \phi_1}{\partial z^2} \right) - \gamma \phi_1. \tag{38}$$

Subjected to the boundary conditions:

$$u_1 = 0, \quad v_1 = -\cos \pi z, \quad w_1 = 0, \quad \theta_1 = 0 = \phi_1 \quad \text{at } y = 0, \tag{39}$$

$$u_1 \rightarrow 0, \quad v_1 \rightarrow 0, \quad w_1 = 0, \quad \theta_1 \rightarrow 0, \quad \phi_1 \rightarrow 0, \quad p_1 \rightarrow 0 \quad \text{as } y \rightarrow \infty \tag{40}$$

Solutions of Zeroth-Order Equations

The solutions of Eqs. (27–30) under the conditions (31), (32) are

$$v_0 = -1 \tag{41}$$

$$\phi_0 = e^{-\lambda y}, \tag{42}$$

$$\theta_0 = (1 + \Lambda_1) e^{-\frac{Pr Re}{\Lambda} y} - \Lambda_1 e^{-\lambda y}, \tag{43}$$

$$u_0 = A_0 e^{-\xi y} + A_4 e^{-\gamma y} + A_5 e^{-\lambda y}. \tag{44}$$

Cross-Flow Solution

To find out the solution of Eqs. (33), (35), and (36) for v_1 , w_1 , and p_1 , we consider the following transformations

$$v_1 = -\pi v_{11}(y)\cos\pi z, \tag{45}$$

$$w_1 = v'_{11}(y)\sin\pi z, \tag{46}$$

$$p_1 = \text{Re}^2 p_{11}(y)\cos\pi z. \tag{47}$$

Here “prime” denotes the differentiation with respect to y .

On substitution of Eqs. (45–47), Eq. (33) is trivially satisfied, and Eqs. (35) and (36) transform to the following form

$$v''_{11} + \text{Re} v'_{11} - \pi^2 v_{11} = -\frac{\text{Re}}{\pi} p'_{11}, \tag{48}$$

$$v'''_{11} + \text{Re} v''_{11} - (\pi^2 + M \text{Re}^2)v'_{11} = -\text{Re} \pi p_{11}. \tag{49}$$

with relevant boundary conditions

$$v_{11} = \frac{1}{\pi}, \quad v'_{11} = 0 \quad \text{at} \quad y = 0, \tag{50}$$

$$v_{11} \rightarrow 0, \quad v'_{11} \rightarrow 0, \quad p_{11} \rightarrow 0 \quad \text{as} \quad y \rightarrow \infty. \tag{51}$$

Subjecting to the boundary conditions (50) and (51), the solution of the Eqs. (48) and (49) are obtained as follows

$$v_{11} = K_0 \left(\bar{\eta} e^{-\eta y} - \eta e^{-\bar{\eta} y} \right), \tag{52}$$

$$p_{11} = \frac{K_0 \eta \bar{\eta}}{\pi \text{Re}} \left(\eta_1 e^{-\eta y} + \bar{\eta} e^{-\bar{\eta} y} \right). \tag{53}$$

Therefore, the solutions for the velocity components v_1 , w_1 and pressure p_1 are as follows

$$v_1 = -\pi K_0 \left(\bar{\eta} e^{-\eta y} - \eta e^{-\bar{\eta} y} \right) \cos\pi z, \tag{54}$$

$$w_1 = K_0 \eta \bar{\eta} \left(e^{-\bar{\eta} y} - e^{-\eta y} \right) \sin\pi z, \tag{55}$$

$$p_1 = \frac{\text{Re} K_0 \eta \bar{\eta}}{\pi} \left(\eta_1 e^{-\eta y} + \bar{\eta} e^{-\bar{\eta} y} \right) \cos\pi z. \tag{56}$$

Solutions for First Order Velocity, Temperature, and Concentration Field

To obtain the solutions for u_1, θ_1 , and ϕ_1 from the Eqs. (34), (37), and (38), we assume the following expressions for u_1 , θ_1 , and ϕ_1 .

$$u_1 = u_{11} \cos\pi z, \quad \theta_1 = \theta_{11} \cos\pi z, \quad \phi_1 = \phi_{11} \cos\pi z \tag{57}$$

Based on Eq. (57), Eqs. (34), (37), and (38) are transformed to

$$\phi''_{11} + \text{Sc} \text{Re} \phi'_{11} - (\pi^2 + \gamma \text{Sc} \text{Re})\phi_{11} = -\pi \text{Sc} \text{Re} v_{11} \phi'_0, \tag{58}$$

$$\Lambda \theta''_{11} + \text{Pr Re} \theta'_{11} - \pi^2 \Lambda \theta_{11} = -\pi \text{Pr Re } v_{11} \theta'_0 - \text{Pr Du} \left(\phi''_{11} - \pi^2 \phi_{11} \right) - \text{Pr Re } Q_l \phi_{11}, \tag{59}$$

$$u''_{11} + \text{Re } u'_{11} - (\pi^2 + M \text{Re}^2) u_{11} = -\text{Gr Re } \theta_{11} - \text{Gm Re } \phi_{11} - \pi \text{Re } v_{11} u'_0. \tag{60}$$

With the conditions,

$$u_{11} = 0, \quad \theta_{11} = 0, \quad \phi_{11} = 0, \quad \text{at } y = 0, \tag{61}$$

$$u_{11} \rightarrow 0, \quad \theta_{11} \rightarrow 0, \quad \phi_{11} \rightarrow 0, \quad \text{as } y \rightarrow 0. \tag{62}$$

Solving (58–60), subjecting to the conditions (61) and (62), we get.

$$\phi_{11} = \lambda \text{ScRe} \pi K_0 \left[A_8 e^{-\omega y} + A_6 e^{-(\eta+\lambda)y} + A_7 e^{-y(\bar{\eta}+\lambda)} \right]. \tag{63}$$

$$\theta_{11} = F_0 e^{-\bar{\omega}y} + F_1 e^{-y(\eta+\gamma)} + F_2 e^{-y(\eta+\lambda)} + F_3 e^{-(\bar{\eta}+\gamma)y} + F_4 e^{-y(\bar{\eta}+\lambda)} + F_5 e^{-\omega y}. \tag{64}$$

$$u_{11} = I_0 e^{-\alpha y} + I_1 e^{-y(\eta+\xi)} + I_2 e^{-y(\eta+\gamma)} + I_3 e^{-y(\eta+\lambda)} + I_4 e^{-y(\bar{\eta}+\xi)} + I_5 e^{-y(\bar{\eta}+\gamma)} + I_6 e^{-y(\bar{\eta}+\lambda)} + I_7 e^{-\bar{\omega}y} + I_8 e^{-\omega y}. \tag{65}$$

For engineering purposes, the coefficient of skin friction τ , the heat transfer coefficient characterized by Nusselt number Nu , or the rate of mass transfer corresponding to Sherwood number Sh at the plate in the non-dimensional form are as follows

$$\tau = - \left. \frac{\partial u}{\partial y} \right]_{y=0}, \quad \text{Nu} = - \left. \frac{\partial \theta}{\partial y} \right]_{y=0}, \quad \text{and} \quad \text{Sh} = - \left. \frac{\partial \phi}{\partial y} \right]_{y=0}. \tag{66}$$

Results and Discussions

The analytical results obtained in the previous section for velocity, temperature, and concentration, as well as for skin friction, Nusselt number, and Sherwood number, are explored graphically for various parameters that are involved in flow problems and flow characteristics. For the computations, we have fixed the following parameters: $\text{Pr} = 0.71$, which corresponds to air, $\text{Sc} = 0.6$ refers to the water vapor diffused in dry air, and $\epsilon = 0.01$, $z = 0$, $\text{Gr} = 5 = \text{Gm}$ are chosen arbitrarily.

Figure 2 reveals that escalating the value of the Dufour number Du improves the velocity profiles. As the Dufour effect intensifies, the thermal buoyancy force within the velocity field strengthens, leading to an acceleration of fluid velocity.

Figure 3 illustrates that the fluid velocity within the boundary layer region is reduced by augmenting the magnetic field parameter. This deceleration is attributed to the presence of the Lorentz force, which opposes the fluid motion. The impact of Reynolds number on velocity and temperature distributions are spotted in Figs. 4 and 5, respectively. These figures make it obvious that the velocity and temperature distributions are decreasing functions of the Reynolds number. In general, rising values of the Reynolds number accelerate fluid velocity; however, in our investigation, the reverse phenomena might be seen. This is because, as the

Fig. 2 Velocity profiles for distinct Du

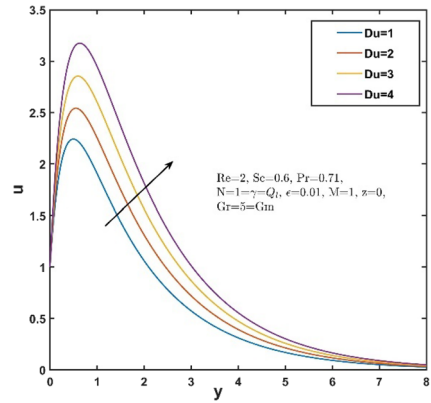
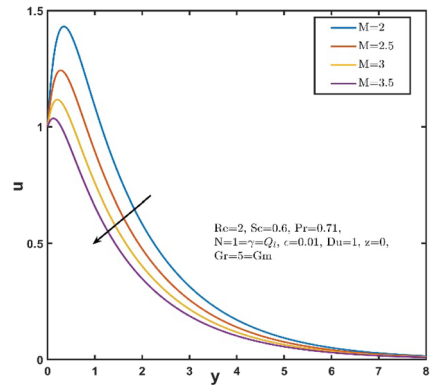


Fig. 3 Velocity profiles for distinct M



Reynolds number grows, the suction effect takes precedence over viscosity, causing the fluid velocity to decrease.

The effects of the radiation absorption parameter Q_l on fluid velocity and temperature are highlighted in Figs. 6 and 7, respectively. These outcomes indicate that velocity and temperature distributions accelerate due to distinct augmenting values of radiation absorption Q_l . Physically, as Q_l is raised, conduction over absorption radiation becomes more dominant. Consequently, this amplifies the buoyancy force and leads to an increase in the thickness of both the hydrodynamic and thermal boundary layers. The influence of the Dufour number Du on temperature distributions is portrayed in Fig. 8. It can be seen from this figure that fluid temperature enhances with increasing Dufour number Du . As we increase the magnitude of Du , the concentration gradients within the temperature field become more pronounced. This results in an elevation of temperature and an expansion of the thermal boundary layer's thickness.

Figures 2, 4, 5, 6, 7, 8 further demonstrates that the temperature and fluid velocity both first rise in a thin layer next to the plate before falling asymptotically and tend to their minimum value at $y = 0$, demonstrating that the buoyancy force has a significant impact on the flow close to the plate and that this impact is negligible in the free stream.

The concentration distributions for distinct values of chemical reaction γ and Reynolds number Re are displayed in Figs. 9 and 10. These results reveal that the concentration profiles

Fig. 4 Velocity profiles for distinct Re

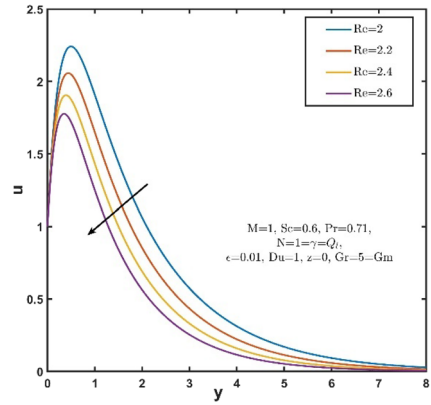


Fig. 5 Temperature profiles for distinct Re

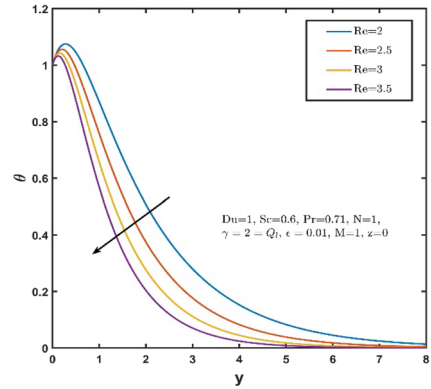
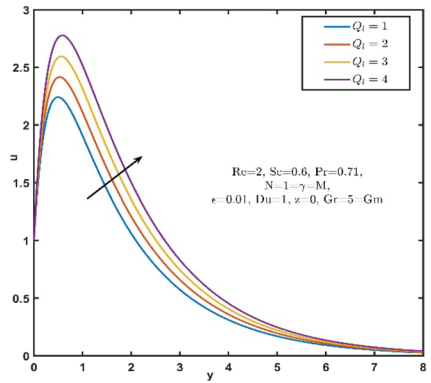


Fig. 6 Velocity for different Q_i



are inversely proportional with chemical reaction parameter γ and Reynolds number Re . The primary explanation is that as chemical reaction parameters increase, the number of solute molecules experiencing chemical reactions rises, which causes a decline in the concentration field. As an outcome, a destructive chemical reaction dramatically minimizes the thickness of the solutal boundary layer.

Fig. 7 Temperature for different Q_l

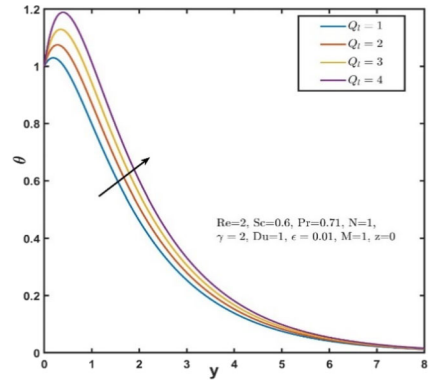
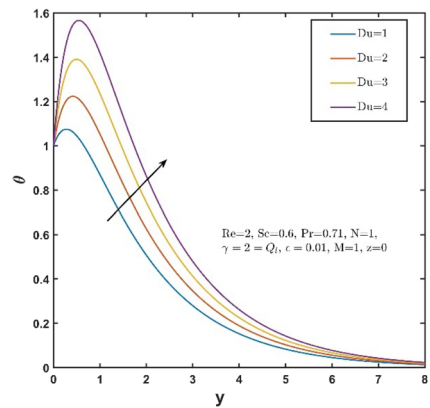


Fig. 8 Temperature for distinct Du



The effects of the Dufour effect (Du), radiation absorption parameter Q_l , and magnetic parameter M on skin friction coefficients are illustrated in Figs. 11, 12, 13. These figures reveal that the shear stress or drag force experienced by the plate is increased due to the presence of the Dufour effect and radiation absorption effect. However, the shear stress or drag force is reduced when the magnetic field is applied.

Figures 14 and 15 clearly indicate that the heat transfer rate, represented by the Nusselt number, demonstrates an upward trend for both the radiation absorption effect and the Dufour effect. These outcomes reflect that heat transfer by convection plays a more significant role than heat transfer by conduction for both the radiation absorption and the Dufour effect.

Figures 16 and 17 assert that the Sherwood number, which measures the rate of mass transfer at the plate, increases for both the chemical reaction parameter γ and Schmidt number Sc. These findings explored the fact that, under the impact of a chemical reaction and Schmidt number, mass transfer by convection is faster than mass transfer by diffusion. Figures 11, 12, 13, 14, 15, 16, 17 further indicate that the growing value of the Reynolds number shrinks the skin friction while increasing the Nusselt and Sherwood numbers. Physically, it reveals that low viscosity slows the momentum transfer rate while boosting heat and mass transfer rates at the plate.

Fig. 9 Concentration for distinct γ

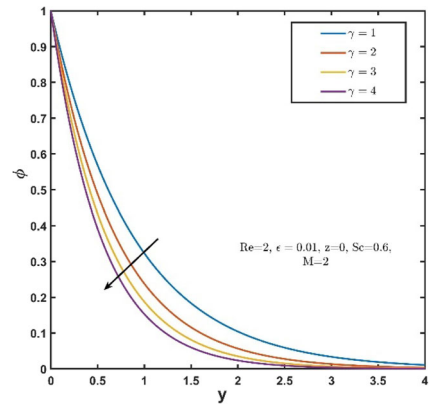


Fig. 10 Concentration profiles for Re

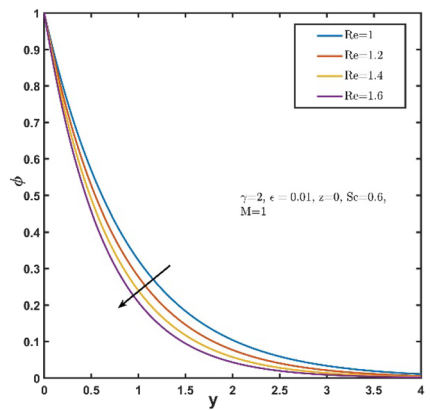


Fig. 11 Impact of Du on skin friction

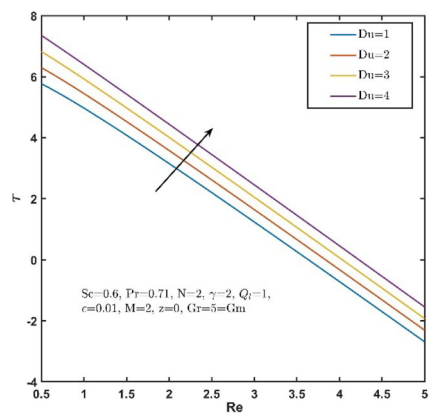


Fig. 12 Impact of Q_I on skin friction

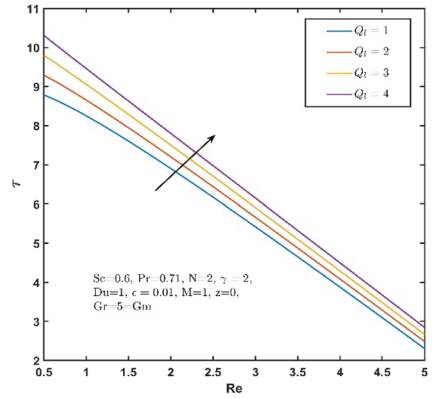


Fig. 13 Impact of M on skin friction

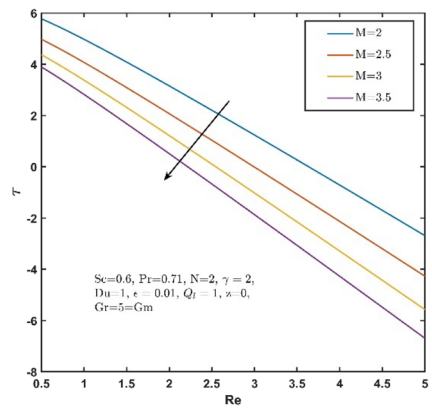


Fig. 14 Impact of Q_I on Nusselt number

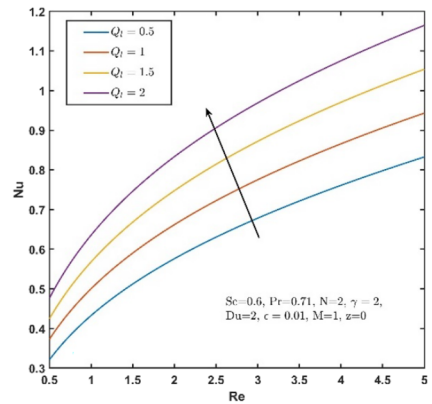


Fig. 15 Impact of Du on Nusselt number

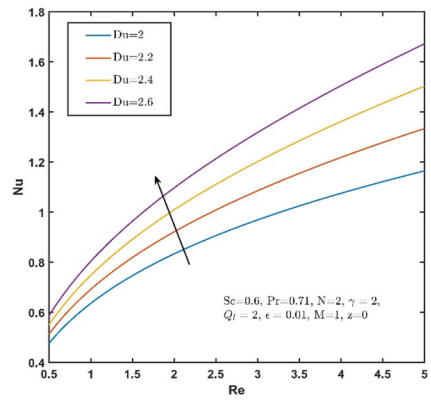


Fig. 16 Sherwood number for γ

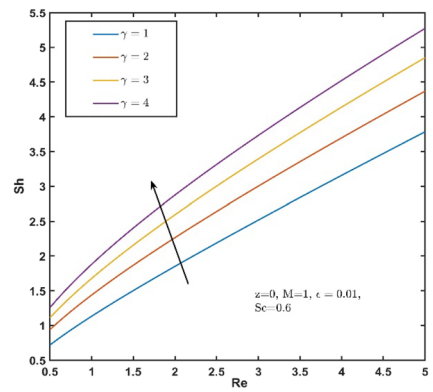
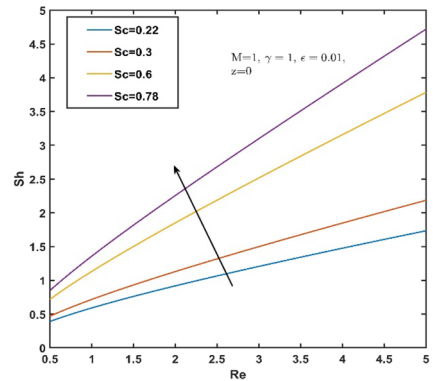


Fig. 17 Sherwood number for Sc



Conclusions

This theoretical study investigates how radiation absorption and diffusion thermo affect a three-dimensional MHD convective flow of a radiating fluid with sinusoidal suction velocity and chemical reaction. The perturbation technique is employed to compute the set of

governing equations. The previous section includes a graphical illustration of the effects of different factors on velocity, temperature, concentration, skin friction, and Nusselt and Sherwood numbers. Based on the previous results and discussion section, some of the significant findings of our study are as follows:

- The growing values of the Dufour number and radiation absorption parameter accelerate the fluid velocity and temperature profiles within the boundary layer region.
- As the Reynolds number expands, the hydrodynamic, thermal, and solutal boundary layer thickness shrinks asymptotically.
- Both the drag force and the rate of heat transfer at the wall are accelerated by the existence of radiation absorption and Dufour effects.
- The amplification of the chemical reaction parameter has accelerated the mass transfer rate at the plate.
- Additionally, it can be identified that the drag force at the wall asymptotically declines as the Reynolds number rises, although the rate of heat and mass transfer exhibits a completely opposite behaviour.

Author Contributions Author A contributions: Conceptualization, formal analysis, methodology, investigation. Author B contributions: Software, investigation, writing-original draft.

Funding There is no funding support for this study.

Data Availability Not applicable.

Declarations

Conflict of interest The authors declare that they don't have any conflict of interest.

Appendix I

$$\lambda = \frac{Sc Re + \sqrt{(Re Sc)^2 + 4\gamma Re Sc}}{2}, \lambda_1 = \frac{1 + \sqrt{1 + 4M}}{2},$$

$$\bar{\lambda}_1 = \frac{1 - \sqrt{1 + 4M}}{2}, \xi = Re\lambda_1, \bar{\xi} = Re\bar{\lambda}_1,$$

$$\Lambda = 1 + \frac{4}{3N}, \Lambda_0 = Pr Du\lambda^2 + Q_I Pr Re, \lambda_1 = \frac{\Lambda_0}{\lambda^2 \Lambda - Pr Re \lambda}, \gamma_1 = \frac{Pr Re}{\Lambda},$$

$$\eta = \frac{\xi + \sqrt{\xi^2 + 4\pi^2}}{2}, \bar{\eta} = \frac{\bar{\xi} - \sqrt{\bar{\xi}^2 + 4\pi^2}}{2},$$

$$K_0 = \frac{1}{\pi(\bar{\eta} - \eta)}, \eta_1 = \eta^2 - \eta Re - (\pi^2 + M Re^2),$$

$$\bar{\eta}_1 = -\bar{\eta}^2 + \bar{\eta} Re + (\pi^2 + M Re^2), \omega = \frac{Sc Re + \sqrt{(Sc Re)^2 + 4(\pi^2 + \gamma Sc Re)}}{2},$$

$$\bar{\omega} = \frac{Pr Re + \sqrt{(Pr Re)^2 + 4\Lambda^2 \pi^2}}{2}, R(D) = D^2 + Re D - M Re^2,$$

$$A_1 = \frac{1 + \Lambda_1}{R(-\gamma_1)}, A_2 = \frac{\Lambda_1}{R(-\lambda)},$$

$$\begin{aligned}
 A_3 &= \frac{1}{R(-\lambda)}, \quad A_0 = 1 + \text{Gr Re } (A_1 - A_2) + \text{Gm Re } A_3, \quad A_4 = -\text{Gr Re } A_1, \\
 A_5 &= \text{Re } (\text{Gm } A_2 - \text{Gr } A_3), \quad f(D) = D^2 + \text{Sc Re } D - (\pi^2 + \gamma \text{Sc Re}), \quad A_6 = \frac{\bar{\eta}}{f(-\bar{\eta} - \lambda)}, \\
 A_7 &= \frac{\eta}{f(-\bar{\eta} - \lambda)}, \quad A_8 = -A_6 - A_7, \quad \gamma_2 = \text{Pr Re } \pi K_0, \quad B_1 = \gamma_2 \bar{\eta} \gamma_1 (1 + \Lambda_1), \\
 B_2 &= -\gamma_2 \bar{\eta} \Lambda_1 \lambda, \quad B_3 = -\gamma_2 \eta \gamma_1 (1 + \Lambda_1), \quad \gamma_3 = \gamma_2 \text{Du Sc } \lambda, \quad B_5 = -\gamma_3 \omega^2 A_8, \\
 B_6 &= -\gamma_3 (\eta + \lambda)^2 A_6, \quad B_7 = -\gamma_3 (\bar{\eta}^2 + \lambda)^2 A_7, \quad \Gamma_0 = \text{Pr } (\pi^2 \text{Du} - \text{Re } Q_l), \\
 \Gamma_1 &= \Gamma_0 \lambda \pi \text{Re Sc } K_0, \quad B_8 = \Gamma_1 A_8, \quad B_9 = \Gamma_1 A_6, \\
 B_{10} &= \Gamma_1 A_7, \quad \Omega(D) = \Lambda D^2 + \text{Pr Re } D - \Lambda \pi^2, \\
 E_1 &= B_2 + B_6 + B_9, \quad E_2 = B_4 + B_7 + B_{10}, \\
 E_3 &= B_5 + B_8, \quad F_1 = \frac{B_1}{\Omega(-\eta - \gamma_1)}, \quad F_2 = \frac{E_1}{\Omega(-\eta - \lambda)}, \\
 F_3 &= \frac{B_3}{\Omega(-\bar{\eta} - \gamma_1)}, \quad F_4 = \frac{E_2}{\Omega(-\bar{\eta} - \gamma_1)}, \\
 F_5 &= \frac{E_3}{\Omega(-\omega)}, \quad F_0 = -\sum_{i=1}^5 F_i, \quad \Gamma_2 = \pi \text{Re } K_0, \\
 \alpha &= \frac{\text{Re} + \sqrt{\text{Re}^2 + 4(\pi^2 + M \text{Re}^2)}}{2}, \quad G_1 = \Gamma_2 \bar{\eta} \xi A_0, \\
 G_2 &= \Gamma_2 \bar{\eta} \gamma_1 A_4, \quad G_3 = \Gamma_2 \bar{\eta} \lambda A_5, \\
 G_4 &= -\Gamma_2 \eta \xi A_0, \quad G_5 = -\Gamma_2 \eta \gamma_1 A_4, \quad G_6 = -\Gamma_2 \eta \lambda A_5, \\
 G_7 &= -\text{Gr Re } F_0, \quad G_8 = -\text{Gr Re } F_1, \quad G_9 = -\text{Gr Re } F_2, \\
 G_{10} &= -\text{Gr Re } F_3, \quad G_{11} = -\text{Gr Re } F_4, \quad G_{12} = -\text{Gr Re } F_5, \\
 \Gamma_3 &= \text{Gm Re}^2 \lambda \pi \text{Sc } K_0, \quad G_{13} = -\Gamma_3 A_8, \quad G_{14} = -\Gamma_3 A_6, \quad G_{15} = \Gamma_3 A_7, \\
 G_{16} &= G_2 + G_8, \quad G_{17} = G_3 + G_9 + G_{14}, \quad G_{18} = G_5 + G_{10}, \quad G_{19} = G_6 + G_{11} + G_{15}, \\
 G_{20} &= G_{12} + G_{13}, \quad G(D) = D^2 + \text{Re } D - (\pi^2 + M \text{Re}^2), \quad I_1 = \frac{G_1}{G(-\eta - \xi)}, \\
 I_2 &= \frac{G_{16}}{G(-\eta - \gamma_1)}, \quad I_3 = \frac{G_{17}}{G(-\eta - \lambda)}, \quad I_4 = \frac{G_4}{G(-\bar{\eta} - \xi)}, \\
 I_5 &= \frac{G_{18}}{G(-\bar{\eta} - \gamma_1)}, \quad I_6 = \frac{G_{19}}{G(-\bar{\eta} - \lambda)}, \\
 I_7 &= \frac{G_7}{G(-\omega)}, \quad I_8 = \frac{G_{20}}{G(-\omega)}, \quad I_0 = -\sum_{k=1}^8 I_k
 \end{aligned}$$

References

1. Riaz, M.B., Maryam Asgir, A.A., Zafar, S.Y.: Combined effects of heat and mass transfer on MHD free convective flow of maxwell fluid with variable temperature and concentration. *Math. Probl. Eng.* **2021**, 1–36 (2021). <https://doi.org/10.1155/2021/6641835>
2. Javaherdeh, K., Nejad, M.M., Moslemi, M.: Natural convection heat and mass transfer in MHD fluid flow past a moving vertical plate with variable surface temperature and concentration in a porous medium. *Eng. Sci. Technol. Int. J.* **18**(3), 423–431 (2015)
3. Mahanthesh, B., Gireesha, B.J., Gorla, R.S.R.: Heat and mass transfer effects on the mixed convective flow of chemically reacting nanofluid past a moving/stationary vertical plate. *Alexandria Eng. J.* **55**(1), 569–581 (2016)
4. Kataria, H., Patel, H.: Heat and mass transfer in magnetohydrodynamic (MHD) casson fluid flow past over an oscillating vertical plate embedded in porous medium with ramped wall temperature. *Propuls. Power Res.* **7**(3), 257–267 (2018)
5. Chamkha, A.J., Rashad, A.M.: Unsteady heat and mass transfer by MHD mixed convection flow from a rotating vertical cone with chemical reaction and Soret and Dufour effects. *Can. J. Chem. Eng.* **92**(4), 758–767 (2014)
6. Veera Krishna, M., Swarnalathamma, B.V., Prakash, J.: Heat and mass transfer on unsteady MHD oscillatory flow of blood through porous arteriole. In: Singh, M.K., Kushvah, B.S., Seth, G.S., Prakash, J. (eds.) *Applications of Fluid Dynamics*, pp. 207–224. Springer Singapore, Singapore (2018). https://doi.org/10.1007/978-981-10-5329-0_14
7. Ahmed, N.: MHD convection with solet and dufour effects in a three-dimensional flow past an infinite vertical porous plate. *Can. J. Phys.* **88**(9), 663–674 (2010)
8. Zafar, M., Rana, M.A., Latif, A.: Three-dimensional fluctuating flow of a second-grade fluid along an infinite horizontal plate with periodic suction. *Math. Probl. Eng.* **2022**, 1–17 (2022). <https://doi.org/10.1155/2022/3509721>
9. Rana, M.A., Ali, Y., Shoaib, M., Numan, M.: Magnetohydrodynamic three-dimensional couette flow of a second-grade fluid with sinusoidal injection/suction. *J. Eng. Thermophys.* **28**, 138–162 (2019)
10. Jain, N.C., Gupta, P.: Three-dimensional free convection couette flow with transpiration cooling. *J. Zhejiang University-Sci. A* **7**, 340–346 (2006)
11. Rana, M.A., Latif, A.: Three-dimensional free convective flow of a second-grade fluid through a porous medium with periodic permeability and heat transfer. *Bound. Value Probl.* (2019). <https://doi.org/10.1186/s13661-019-1144-x>
12. Ibrahim, F.S., Elaiw, A.M., Bakr, A.A.: Effect of the chemical reaction and radiation absorption on the unsteady MHD free convection flow past a semi-infinite vertical permeable moving plate with heat source and suction. *Commun. Nonlinear Sci. Numer. Simul.* **13**(6), 1056–1066 (2008)
13. Satya Narayana, P.V.: Effects of variable permeability and radiation absorption on magnetohydrodynamic (MHD) mixed convective flow in a vertical wavy channel with traveling thermal waves. *Propuls. Power Res.* **4**(3), 150–160 (2015). <https://doi.org/10.1016/j.jprr.2015.07.002>
14. Hernández, V.R., Zueco, J.: Network numerical analysis of radiation absorption and chemical effects on unsteady MHD free convection through a porous medium. *Int. J. Heat Mass Transfer* **64**, 375–383 (2013). <https://doi.org/10.1016/j.ijheatmasstransfer.2013.03.074>
15. Venkateswarlu, B., Satya Narayana, P.V.: Chemical reaction and radiation absorption effects on the flow and heat transfer of a nanofluid in a rotating system. *Appl. Nanosci.* **5**, 351–360 (2015)
16. Veera Krishna, M.: Radiation-absorption, chemical reaction, hall and ion slip impacts on magnetohydrodynamic free convective flow over semi-infinite moving absorbent surface. *Chin. J. Chem. Eng.* **34**, 40–52 (2021). <https://doi.org/10.1016/j.cjche.2020.12.026>
17. Arifuzzaman, S.M., Khan, M.S., Mehedi, M.F.U., Rana, B.M.J., Ahmmed, S.F.: Chemically reactive and naturally convective high speed MHD fluid flow through an oscillatory vertical porous plate with heat and radiation absorption effect. *Eng. Sci. Technol. Int. J.* **21**(2), 215–228 (2018)
18. Anwar, T., Kumam, P., Baleanu, D., Khan, I., Thounthong, P.: Radiative heat transfer enhancement in MHD porous channel flow of an oldroyd-b fluid under generalized boundary conditions. *Phys. Scr.* **95**(11), 115211 (2020)
19. Kumam, P., Tassaddiq, A., Watthayu, W., Shah, Z., Anwar, T., et al.: Modeling and simulation-based investigation of unsteady MHD radiative flow of rate type fluid; a comparative fractional analysis. *Math. Comput. Simul.* **201**, 486–507 (2022)
20. Anwar, T., Kumam, P., Watthayu, W.: Unsteady MHD natural convection flow of casson fluid incorporating thermal radiative flux and heat injection/suction mechanism under variable wall conditions. *Sci. Rep.* **11**(1), 4275 (2021)

21. Wahid, N.S., Arifin, N.M., Khashi'ie, N.S., Pop, I., Bachok, N., Hafidzuddin, M.E.H.: MHD mixed convection flow of a hybrid nanofluid past a permeable vertical flat plate with thermal radiation effect. *Alexandria Eng. J.* **61**(4), 3323–3333 (2022). <https://doi.org/10.1016/j.aej.2021.08.059>
22. Anwar, T., Khan, I., Kumam, P., Watthayu, W.: Impacts of thermal radiation and heat consumption/generation on unsteady MHD convection flow of an oldroyd-b fluid with ramped velocity and temperature in a generalized darcy medium. *Mathematics* **8**(1), 130 (2020). <https://doi.org/10.3390/math8010130>
23. Eckert, E.R.G., Robert, M. Drake, J.: Analysis of heat and mass transfer. 1987.
24. Waini, I., Ishak, A., Pop, I.: Dufour and sores effects on al₂o₃-water nanofluid flow over a moving thin needle: Tiwari and das model. *Int. J. Numer. Methods Heat Fluid Flow* **31**(3), 766–782 (2021)
25. Postelnicu, A.: Influence of a magnetic field on heat and mass transfer by natural convection from vertical surfaces in porous media considering sores and dufour effects. *Int. J. Heat Mass Transf.* **47**(6–7), 1467–1472 (2004)
26. Kandasamy, R., Hayat, T., Obaidat, S.: Group theory transformation for sores and dufour effects on free convective heat and mass transfer with thermophoresis and chemical reaction over a porous stretching surface in the presence of heat source/sink. *Nucl. Eng. Des.* **241**(6), 2155–2161 (2011)
27. Kune, R., Naik, H.S., Reddy, B.S., Chesneau, C.: Role of nanoparticles and heat source/sink on MHD flow of cu-h₂o nanofluid flow past a vertical plate with sores and dufour effects. *Math. Comput. Appl.* **27**(6), 102 (2022)
28. Zhao, J., Zheng, L., Zhang, X., Liu, F.: Convection heat and mass transfer of fractional MHD maxwell fluid in a porous medium with sores and dufour effects. *Int. J. Heat Mass Transf.* **103**, 203–210 (2016)
29. Huang, Ch.J., Yih, K.A.: Heat generation and sores–dufour effects on heat and mass transfer in mixed convection flows of power-law fluids about a vhf/vmf plate in porous media: the entire regime. *J. Appl. Mech. Tech. Phys.* **64**(1), 88–97 (2023)
30. Reddy, N.N., Reddy, Y.D., Rao, V.S., Shankar Goud, B., Nisar, K.S.: Multiple slip effects on steady MHD flow past a non-isothermal stretching surface in presence of sores, dufour with suction/injection. *Int. Commun. Heat Mass Transfer* **134**, 106024 (2022)

Publisher's Note Springer Nature remains neutral with regard to jurisdictional claims in published maps and institutional affiliations.

Springer Nature or its licensor (e.g. a society or other partner) holds exclusive rights to this article under a publishing agreement with the author(s) or other rightsholder(s); author self-archiving of the accepted manuscript version of this article is solely governed by the terms of such publishing agreement and applicable law.